Published in final edited form as:
Nanomedicine. 2013 October ; 9(7): 903–911. doi:10.1016/j.nano.2013.01.003.

A chitosan-modified graphene nanogel for noninvasive controlled drug release

Chunyan Wang, PhD[a,b], **Jaya Mallela, PhD**[a,b], **Ujjwala Sree Garapati, MS**[a], **Sowndharya Ravi, MS**[a], **Vignesh Chinnasamy, MS**[a], **Yvonne Girard, MS**[a,b], **Mark Howell, MS**[a,b], and **Subhra Mohapatra, PhD**[a,b,*]

[a]Molecular Medicine Department, Morsani College of Medicine, University of South Florida, Tampa, FL, USA

[b]USF Nanomedicine Research Center, Morsani College of Medicine, University of South Florida, Tampa, FL, USA

Abstract

A near infrared (NIR) triggered drug delivery platform based on the chitosan-modified chemically reduced graphene oxide (CRGO) incorporated into a thermosensitive nanogel (CGN) was developed. CGN exhibited an NIR-induced thermal effect similar to that of CRGO, reversible thermo-responsive characteristics at 37–42 °C and high doxorubicin hydrochloride (DOX) loading capacity (48 wt%). The DOX loaded CGN (DOX-CGN) released DOX faster at 42 °C than at 37 °C. The fluorescence images revealed DOX expression in the cytoplasm of cancer cells when incubated with DOX-CGN at 37 °C but in the nucleus at 42 °C. Upon irradiation with NIR light (808 nm), a rapid, repetitive DOX release from the DOX-CGN was observed. Furthermore, the cancer cells incubated with DOX-CGN and irradiated with NIR light displayed significantly greater cytotoxicity than without irradiation owing to NIR-triggered increase in temperature leading to nuclear DOX release. These results demonstrate CGN's promising application for on-demand drug release by NIR light.

Keywords

NIR; Graphene; Thermosensitive; Drug release; Photothermal; Nanogel

Noninvasive externally-controlled drug release systems are attractive since they allow remote, repeatable, and reliable switching on or off of drug release based on need. The complete noninvasive remote-controlled drug delivery system comprises of drug, an external stimulus, stimulus-sensitive materials, and stimulus-responsive carriers. The external stimulus can be light,[1–3] a magnetic field,[4,5] ultrasound[6] or radio-frequency.[7,8] An NIR light-triggered release system utilizes the photothermal property of a material, which absorbs NIR light and converts it into heat thereby inducing the drug release from a thermo-sensitive carrier. Photothermal materials with strong optical absorbance in the NIR include various gold nanostructures (gold nanorods, gold nanocages, hollow gold nanospheres, gold nanoshells), carbon materials (carbon nanotubes, graphene), or conducting polymers that have been extensively studied for photothermal therapy.[9–12] Gold nanoparticles, gold nanorods, and gold nanocages have been studied for the NIR-triggered drug release by

*Corresponding author. University of South Florida, Molecular Medicine Department, Tampa, Florida, USA. smohapa2@health.usf.edu (S. Mohapatra).

incorporation into thermo-responsive materials.[1,6,13] However, none of these delivery systems have been advanced to clinical trials yet.

Two-dimensional graphene has received considerable attention in biomedical applications in the past few years owing to its high mechanical strength, pH sensitivity, photosensitivity and low toxicity.[10,14,15] Graphene shows higher photothermal sensitivity than carbon nanotubes (CNT) and was shown to be highly effective in photothermal therapy for cancer.[9–12] In addition, the highly efficient photothermal conversion of graphene enabled graphene oxide/pluronic hydrogel to undergo rapid gelation by NIR laser irradiation.[16,17] Whether chemically reduced graphene oxide (CRGO) is capable of acting as a photosensitive material for remote-controlled drug delivery has not been investigated yet.

A thermo-responsive carrier is another important requirement of the light-triggered remote-controlled drug delivery system. Poly(N-isopropylacrylamide) (PNIPAM) undergoes a reversible discontinuous phase transition in water, changing from hydrophilic (swelling) to hydrophobic (shrinking) in response to a temperature change. This thermosensitive property of PNIPAM has been utilized for switchable drug delivery systems via incorporation of stimulus-sensitive materials. The PNIPAM hydrogels containing gold nanorods or gold-gold sulfide nano-shells, or PNIPAM nanogel-incorporated ethyl cellulose membranes containing magnetic nanoparticles demonstrate drug release resulting from the shrinkage of gel due to the heat produced by absorption of light or magnetic triggering.[4,18–20] However, it is difficult to obtain stable nanoparticle dispersions in gels without disturbing the thermosensitivity of the hydrogel matrix. To improve the dispersion stability of the nanoparticles in the gel, Wang et al. enclosed gold nanoparticles inside a PNIPAM hydrogel with Au-reactive functional groups.[21] Shiotani et al. reported stable incorporation of gold nanorods into PNIPAM hydrogels by replacement of the surfactant on the surface of gold nanorods with thiol-terminated PEG.[18] However, such modification of the network polymers resulted in a shift in the volume-phase transition temperature and a reduced sharpness of the volume-phase transition behavior. Goreliko et al. prepared gold nanorod embedded PNIPAM-co-acrylic acid microgels by attractive electrostatic forces between the negatively charged microgel and positively charged gold nanorods.[22] However, for *in vivo* delivery, hybrid microgels cannot be used for systemic injection because their size is too large to circulate in the blood. To create a nanoscale delivery system, Kawano et al. applied PNIPAM onto the surface of a silica-coated gold nanorod followed by silica etching to obtain the hollow PNIPAM nanocapsule containing a single gold nanorod.[23] However, they did not test the drug delivery capability. Here, in order to achieve stable incorporation of CRGO to nanogel, CRGO was grafted with positively charged hydrophilic chitosan, which can increase the dissolution of nanoparticles and prevent the aggregation.[24]

In this study, we exploited the high photothermal sensitivity of CRGO as the stimulus and thermosensitive nanogel as the carrier for remote controlled release of the anticancer drug, doxorubicin hydrochloride (DOX). The CGN was prepared from acrylated chitosan CRGO, N-isopropylacrylamide and PEG diacrylate, and then loaded with DOX. The morphology, hydrodynamic diameter, photothermal property, reversible thermosensitivity, and cytotoxicity of CGN were characterized with TEM, DLS, NIR laser, UV-vis, and PrestoBlue assay, respectively. After the evaluation of the drug loading capacity, thermosensitive release, and NIR-light-triggered drug release of CGN, the uptake of DOX-CGN and subcellular localization were tested in cancer cells using confocal laser scanning microscopy. Finally, the drug delivery efficiency of DOX-CGN was also evaluated on cancer cells by cell viability assay.

Methods

Materials

Graphene oxide 0.5% water solution was purchased from Angstron Materials Inc., OH, USA. Water soluble chitosan (Mw 10 kDa) was donated by Transgenex Nanobiotech Inc. Poly (sodium 4-styrenesulfonate) (PSS, Mw 70,000), N-isopropylacrylamide (NIPAM), acrylic acid anhydrous, polyethylene glycol-diacrylate (PEG-diacrylate), ethyl (dimethylaminopropyl) carbodiimide (EDC), N-hydroxysuccinimide (NHS) were bought from Sigma-Aldrich (St Louis, MO, USA).

Preparation of CRGO with acrylated chitosan

To prepare acrylated chitosan modified CRGO, firstly, CRGO-COOH was prepared according to the reported procedure with minor modification.[25,26] PSS-coated reduced GO sheets were prepared by reducting 50 mg GO (1 mg ml^{-1}) in the presence of PSS (15 mg ml^{-1}) and 1.5 ml hydrazine under refluxing at 100 °C.[25] The brown color of the GO suspension was changed to black CRGO suspension. After cooling to room temperature, 1.2 g NaOH and 1.0 g chloroacetic acid were added to the GO-PSS solution and sonicated with 2510 Branson sonicator for 3 h[26] to convert the OH groups to COOH via conjugation of acetic acid moieties giving CRGO-COOH. To conjugate chitosan to the CRGO-COOH, 1 mg/ml CRGO-COOH suspensions (4 ml) were activated with EDC (30 mg) and NHS (30 mg) in 1 ml water for 30 min, and added to 10 ml of water-soluble chitosan solution (10 mg/ml) in water. The reaction was kept for 3 h at room temperature before dialyzing in a 12 kDa molecular weight-cutoff dialysis bag for 2 days at room temperature against water. Finally, acrylated chitosan-CRGO was prepared by adding 1 ml EDC and NHS activated acrylic acid to 10 ml the above chitosan-CRGO solution. After reacting for 3 h, the solution was purified by dialysis in a 1 kDa molecular weight-cutoff dialysis bag for 2 days at room temperature against water.

Preparation of CGN

300 mg of NIPAM, 50 μl of PEG-diacrylate, and 1 ml of acrylated chitosan-CRGO (10 mg/ml) were added to 25 ml of nano-pure water in a three-necked flask. The solution was purged with argon gas for 30–45 s, and 25 ml of APS (53 mg in 25 ml) was added drop wise. The solution changed from colorless to white in 30 min and kept reacting for 4 h. The sample solution was purified by dialysis in 1 kDa molecular weight cutoff dialysis bag for 2 days at room temperature against water. Some of the solution was kept at room temperature as a further test of thermal sensitivity. The rest of purified solution was freeze-dried and kept at 4 °C.

Characterization

The temperature dependence of the phase transition of CGN was determined turbidimetrically (at 650 nm) by a Lambda 35 UV/vis spectroscope (Perkin-Elmer, USA) fitted with a 1-cm optical path length quartz cell. The dispersions were diluted and heated from 35 to 45 °C at a heating rate of 1°C min^{-1}. The hydrodynamic particle sizes of CGN were measured from 35 °C to 42 °C using a DynaPro DLS plate reader (Wyatt Technology, Germany). The morphology of the CGN was determined by transmission electron microscopy (TEM).

The photothermal properties of CRGO and CGN were tested using an NIR Laser Module source (RLDH808-1200-5, Roithner Laserthchnik Gmbh, Vienna, Austria) emitting at 808 nm (900 mW/cm^2). The suspension (2 ml) in a 15 ml conical-bottom centrifuge tube was irradiated for 5.5 min. The temperature increase was measured by a thermocouple inserted into the solution.

Drug loading and release

Freeze-dried CGN nanoparticles (1 mg) were mixed with different concentrations of DOX solution at 4 °C overnight. The solution was placed in a dialysis bag (1 kDa MWCO) against water to remove free DOX at room temperature for two hours. The dialysis bag with DOX-loaded CGN was placed into 30 ml phosphate-buffered saline (pH 7.4) in a 50 ml centrifuge tube. The tube was placed into a 37 °C water bath or 42 °C water bath. At various times, 2 ml was withdrawn from the tubes to measure DOX absorbance at 485 nm. The concentration of DOX was calculated from a standard curve of known DOX concentrations.

To test the NIR triggered DOX release, a 2 ml DOX-CGN suspension (1 mg/ml) was irradiated with the 808-nm NIR light (900 mW/cm^2) over a period of 3 min. After temperature of the suspension was cooled down to the room temperature, aliquots were withdrawn from the test tube and centrifuged at 10,000 rpm for 10 min, and the released free DOX was quantified by measuring DOX absorption at 485 nm using UV–vis.

Determination of DOX-CGN cell uptake

For cellular uptake and subcellular localization tests, cells were seeded (60,000 cells per chamber) in four-well chamber CellView™ culture dish (Griener, Bio-one) and grown at 37 °C overnight. The plates were put in 3i live cell pathology device at 37 °C or 42 °C. We chose 42 °C, which is higher than the low critical solution temperature (LCST) of CGN as the *in vivo* test temperature, because of the cooling capacity of the bloodstream and perspiration. After the samples (4 μM) were added to the cells, the fluorescent images were taken at 0 min, 30 min and 60 min with 3i Olympus Spinning Disk Confocal Microscope (laser, 488 nm). The fluorescent characteristic of DOX (λex=470 nm, λem=590 nm) was used to monitor the cell uptake and drug release process of DOX or DOX-CGN at 37 °C and 42 °C.

Cytotoxicity of DOX-CGN

To determine cell viability after treatment with DOX alone or DOX-CGN, cells (15,000 per well) were allowed to adhere to a 96-well plate overnight before adding DOX or DOX-CGN. For testing the thermo-release of DOX from DOX-CGN, the cells were incubated with DOX-CGN or free DOX at 37 °C or 42 °C for 30 min after which the plates were returned to 37 °C for three days. The viability was determined by PrestoBlue assay. Viability values were calculated as the fraction of treated cells/untreated cells.

NIR-light-triggered cellular uptake and cytotoxicity

For NIR-triggered cellular uptake and subcellular localization tests, cells were seeded (1.50×10^5) in 6-well culture dish and grown at 37 °C overnight. Cells were incubated with CGN, DOX-CGN or PBS for two hours and then trypsinized, resuspended, and washed by centrifugation at 400*g* into 4 ml DMEM media containing 10% FBS. 2 ml of each cell suspension (PBS, CGN, DOX-CGN) was irradiated for 3 min in a 15 ml tube with an 808 nm laser at a power of 900 mW/cm^2. Immediately after irradiation, cells were washed one more time, centrifuged and resuspended in DMEM media. Finally, 2×10^4 cells per well were plated in an 8-well chamber slide. After 8 h incubation, cells were washed with PBS and fixed in a solution of 4% paraformaldehyde in PBS at 37 °C for 10 min and then mounted in VectaShield (Vector Laboratories) containing fluorescent 4′, 6-diamidino-2-phenylindole (DAPI). Images were acquired with a confocal microscope. The remaining cells were plated into a 96-well plate for evaluating cytotoxicity using PrestoBlue assay.

Statistics

Statistical analysis was performed using Student's *t* test. A *P* value of less than 0.05 was considered as a statistically significant difference.

Results

Preparation and characterization of CGN

To prepare CGN, we first synthesized CRGO, as described.[27] Next, CRGO sheets were functionalized with carboxylic acid (COOH) moieties,[26] which in turn were covalently bound with chitosan via the amide bond in the presence of EDC and NHS. To prevent coagulation, the chitosan functionalized CRGO sheet was further reacted with acrylic acid to obtain the acrylated chitosan-CRGO monomer. The acrylated chitosan-CRGO monomers were copolymerized with NIPAM and PEG-diacrylate crosslinker to form a nanogel (Figure 1) instead of being physically dispersed inside the gel.

The particle morphology of CGN is spherical and the particle size distribution is monodisperse (Figure 2, *A*). Figure 2, *B* shows the uniformly dispersed graphene inside the nanogel. UV–vis spectroscopy was used to analyze the optical absorption of CGN and DOX-CGN compared to CRGO (Figure 2, *C*). Similar to PEG-functionalized nanographene sheets,[10] CGN exhibited strong optical absorption. Compared to the CRGO, the apparent increases of absorption of CGN and DOX-CGN in the visible region (400–700 nm) were due to light scattering by the PNIPAM nanogel or DOX absorption.

The photothermal responsiveness of CRGO, CGN suspension, and water is shown in Figure 2, *D*. In contrast to the water sample, the CRGO and CGN suspension showed a rapid increase of temperature in 5.5 min. The heat generating capacity of CGN ($\Delta T \approx 24.5$ °C in 5.5 min) in the same conditions is comparable to CRGO suspension ($\Delta T \approx 26.3$ °C in 5.5 min), but significantly higher than water ($\Delta T \approx 15$ °C in 5.5 min). These data indicate that CRGO and CGN display high photothermal responsiveness.

The temperature-induced change in size of the CGN was measured by DLS (Figure 3, *A*) using heat as the stimulus. The CGN exhibited a thermoresponsive discontinuous phase-transition due to the dehydration of the polymer chains and the collapse of the hydrophilic segments. The diameter of CGN decreased ~220 nm on heating to 40 °C. The size of the dried CGN (35 nm) observed in TEM was much smaller than the size determined by DLS.

The thermosensitive behavior of CGN at physiological temperatures was also evaluated by monitoring the turbidity change of aqueous CGN solutions upon temperature change (Figure 3, *B*). The turbidity of CGN solution increases rapidly with increasing temperature from 39 to 42 °C. When the temperature reaches 42 °C, the nanogel begins to shrink and water molecules are squeezed out of the nanogel. The difference in the refractive index between the nanogel and water increases causing the increased turbidity. During cooling/heating cycles, the turbidity of the sample at 42 °C or 25 °C remained the same (Figure 3, *C*), suggesting that the turbidity changes with temperature were reversible.

Cytotoxicity of CGN

To evaluate the potential application of this reversible thermal responsiveness of CGN, its biocompatibility was assessed by testing for effects of CGN on the viability of a mouse prostate cancer cell line, TRAMP-C1. Supplement Fig S1 shows the viability of TRAMP-C1 cells exposed to different concentrations of CGN, expressed as a percent of cell survival without CGN. There is no decrease in cell viability observed upon exposure to high concentration of CGN. To test for possible effect of nanogel heating on cell viability, the

cells were treated with different concentration of CGN at 42 °C for 30 min and then returned to 37 °C. The viability of cells incubated at 42 °C remained similar to those cultured at 37 °C (Fig. S1). These results demonstrate that no statistically significant decrease of cell viability was observed when TRAMP-C1 cells treated with CGN at 42 °C for 30 min ($p>0.05$).

Drug loading and release

To test the drug-loading capacity, the freeze-dried CGN nanoparticles were added to an aqueous solution of DOX and mixed thoroughly at 4 °C overnight to load the drug. The drug-loading content (wt%) at different DOX starting concentrations is shown in Figure 4, *A*. The drug loading content increased with DOX feeding concentration because more drug molecules were available for entrapment. The equilibrium drug loading content was found to be 48 wt% of dry CGN. To determine how temperature influences the release of DOX, DOX-CGN was incubated at 37 °C and 42 °C. Figure 4, *B* shows the time-dependent release profile of DOX at 37 °C and 42 °C. Drug release was more and faster at 42 °C than at 37 °C due to the thermo-sensitive release of DOX. Next, the NIR-light-triggered DOX release from DOX-CGN was tested by treating the DOX-CGN suspension to an NIR laser (808 nm, 900 mW) (Figure 4, *C*), for 5 cycles each of exposure for 3 min followed by a 30 min gap. A fast release of DOX molecules (8.46%) occurred within 3 min after irradiation. In contrast, only 3.33% DOX was released without irradiation. During the second 3 min cycle, 10.58% DOX was released with irradiation compared to 4.60% DOX released without irradiation. There was 12.89% and 14.80% cumulative DOX release during the third and fourth cycle, respectively. The cumulative DOX release reached 18.81% when DOX-CGN was exposed to NIR laser five times with 3-min interval. However, in the absence of irradiation, the cumulative DOX release was leveled off at about 5%.

Cellular uptake and subcellular localization of DOX-CGN

To investigate the DOX release behavior of DOX-CGN in cells at 37 °C and 42 °C, TRAMP-C1 cells were treated with DOX-CGN or free DOX (4 μM). The uptake of DOX by the cells was monitored by taking images at 0, 30 and 60 min after DOX-CGN or free DOX was added (Figure 5, *A* and *B*). At 37 °C, both DOX-CGN and free DOX were internalized into cells after 30 min. After 60 min, an increase in nuclear fluorescence intensity was observed for the free DOX. However, the DOX-CGN showed fluorescence exclusively in the cytoplasm. In contrast, when the cells were incubated at 42 °C for 30 min, an increase in nuclear fluorescence intensity was observed for both free DOX and DOX-CGN. At 37 °C, DOX remained sequestered inside the nanogel after internalization of DOX-CGN but DOX was released from the nanogel at 42 °C and entered the nucleus. Compared to 37 °C, the cells show more internalization of both DOX-nanogel and free DOX at 42 °C.

Cytotoxicity of DOX-CGN against cancer cells in culture

To determine the cytotoxicity of DOX-CGN nanogels at 37 °C and 42 °C, TRAMP-C1 cell viability was tested with different concentrations of DOX-CGN or free DOX at 37 °C (Figure 5, *C*), or at 42 °C (Figure 5, *D*). At 37 °C, the cytotoxicity of DOX-CGN was significantly less than free DOX ($p<0.05$). The IC_{50} value of free DOX and DOX-CGN was 2 μM and 20 μM, respectively. At 42 °C, DOX-CGN showed comparable cytotoxicity to free DOX ($p>0.05$). The IC_{50} of free DOX and DOX-CGN was less than 1 μM.

NIR-light-triggered cellular uptake and cytotoxicity of DOX-CGN

Internalization of the DOX-CGN and its ability to undergo photothermal release inside Lewis lung cancer 1 (LLC1) cells were studied by comparing the confocal fluorescence microscope images of the LLC1 cells incubated with PBS, CGN, and DOX-CGN exposed to

NIR laser (Figure 6, *A*). DOX fluorescence was observed inside the cells treated with DOX-CGN indicating the cellular uptake of the DOX-CGN. No DOX fluorescence was observed in cells treated with PBS or CGN. The fluorescence images revealed that in the irradiated cells, most DOX was located in the nucleus whereas in the non-irradiated cells it was distributed in the cytoplasm. Similar results were observed with TRAMP-C1 cells (Figure 6, *B*).

The effects of DOX-CGN, with or without NIR irradiation, on the viability of LLC1 and TRAMP-C1 cells were compared. As shown in Figure 6, *C* and *D*, a significant difference in cytotoxicity between DOX-CGN combined with NIR irradiation and that of DOX-CGN alone was observed. When LLC1 cells were incubated with DOX-CGN, 77.5% of the cells were viable after 48 h of incubation. However, when cells were incubated with DOX-CGN at the same concentration and irradiated with NIR, only 51.31% of the cells survived. When cells were incubated with CGN or PBS, more than 95% of the cells were viable, regardless of whether the cells were irradiated with the NIR laser suggesting that short time irradiation by itself is not toxic to the cells. Similar findings were observed with TRAMP-C1 cells (Figure 6, *D*).These results indicate that the cytotoxic effect of DOX-CGN upon irradiation was due to the NIR-triggered DOX release, but not owing to irradiation or CGN alone.

Discussion

To develop an NIR-triggered remote-controlled drug release system, the critical material is the photosensitizer with high absorption in the NIR region that can generate heat from light absorption. In the carbon family, materials with high photo-thermal properties in the NIR region for cancer therapy include single-walled carbon nanotubes,[28–30] multiwalled carbon nanotubes,[31] and graphene,[10,32] but not carbon fiber or graphite. It was reported that CRGO shows much (about 6.8 times) higher NIR absorption than graphene oxide.[12,31] Furthermore, the high specific surface area and functional groups of two-dimensional graphene enable facile biological/chemical functionalization. Therefore, we chose CRGO as the photothermal stimulus for a controlled drug release system. By incorporating CRGO into thermosensitive nanogel, we anticipated that the high photo-thermal property of CRGO would result in a drug-delivery system that is highly responsive to NIR laser irradiation. DOX was incorporated into the CGN to demonstrate the NIR-light-triggered release of a widely used anticancer agent.

Figure 1 depicts the synthesis process of the DOX-CGN and proposed mechanism of the NIR-light-triggered release of drugs from nanogel. First, we prepared uniformly dispersed nanoparticles inside the nanogel. Compared to conventional physical mixing, the nanoparticles were uniformly dispersed inside nanogel via chemical bond, which was supported by the TEM studies (Figure 2, *A* and *B*). The CGN nanogels maintained their dispersion stability and exhibited no aggregation or precipitation for 3 to 4 months. To evaluate the photothermal property of the CGN, the temperature changes of CGN suspension upon exposure to NIR were compared with the CRGO suspension. The results indicated that CGN was able to elevate the temperature of water to the similar extent as CRGO alone at the same concentration (Figure 2, *D*). In addition, the UV–vis absorption of CRGO and CGN at 808 nm was almost the same (Figure 2, *C*). Thus, the encapsulation of CRGO into nanogel did not affect the absorption of NIR light and the photothermal conversion capacity of CRGO.

Second, to make CGN nanogel stimulus responsive, thermosensitive PNIPAM was used. The LCST of pure PNIPAM gel crosslinked with N,N′-methylenebisacrylamide (BIS) is 32–34 °C.[1,18] When the temperature is raised above 32 °C, the polymer undergoes a phase transition to a hydrophobic state, causing the gel to shrink. Using the pure PNIPAM

hydrogel as the thermosensitive carrier for controlled drug release *in vivo*, the drug release state will always be 'on'. Therefore, we needed to adjust the LCST above the human body temperature (37 °C) but below the hyperthermia temperature (42 °C) for *in vivo* applications. To tune the LCST of PNIPAM, the hydrophilic monomer acrylamide (AAm) or acrylic acid was copolymerized with PNIPAM.[1,22] Here, the acrylated chitosan graphene is another hydrophilic monomer that was used to adjust the LCST. In addition, the hydrophilic biocompatible crosslinker PEG-diacrylate was used instead of hydrophobic BIS. CGN shows significant reduction in size when temperature changed from 37 °C to 42 °C. This reduced sharpness of the volume phase transition is comparable to the PNIPAM gel coated gold nanorod.[23] In accordance with the size change of CGN upon heating, the turbidity of the CGN also demonstrated the thermosensitve response. These results suggest that the CGN remains swollen (in the 'off' state) at 37 °C, but shrinks (in the 'on' state') above the phase transition temperature.

For successful anticancer drug delivery, the drug carriers have to be constructed not only to respond to a specific stimulus, but also to achieve a high drug loading capacity. For the reported light-triggered remote controlled drug delivery system,[18,22,33] there has been little focus on drug loading capacity, even though drug loading capacity is a bottle-neck issue for the successful development of drug vehicles for potential clinical use. Drug molecules can be incorporated into nanogels through chemical conjugation, physical entrapment during polymerization, or physical diffusion. Compared to the complicated preparation and low bioavailability of chemical conjugation and difficulty of purification of physical entrapment, the physical diffusion method is the simplest and allows for easy purification before drug loading. In our formulation, the hydrophilic DOX molecules diffused to the nanogel during its swelling process. The 48 wt% drug loading content of CGN is significantly higher than the 26 wt% of pH-sensitive pegylated nanogel or 16.14 wt% of mPEG-P (LG-LC) nanogel.[34,35] Compared to 37 °C, more DOX release from our DOX-CGN was seen at 42 °C, which indicated that temperature could be used to control the release of the drug from the nanogel. Next, the DOX-CGN was exposed to the NIR to determine the possibility of NIR-light-triggered drug release. The results showed that the heat generated by absorption of NIR was sufficient to trigger DOX release. The release of DOX from CGN could be readily modulated by controlling the cycles of laser irradiation (Figure 4, *C*). These results suggested that the photothermal effect of CRGO in the nanogel could lead to the controllable DOX release from DOX-CGN. The potential shortage of this release system is difficult to control the same drug amount at different cycle. There was 8.46% cumulative DOX release at the first 3 min irradiation. However, there was a 2.12%, 2.31%, 1.92%, and 1% increase in cumulative release at the second, third, fourth, and fifth irradiation cycle, respectively. The reason for this decrease of the release rate during subsequent irradiation cycles is unclear, and it is in agreement with other reported NIR remote-controlled release systems.[36,37]

The confocal fluorescence images of TRAMP-C1 cells (Figure 5, *A* and *B*) demonstrated that the DOX-CGN was taken up by cells via the endocytic pathway and transported into the endosome. At 37 °C, free DOX was observed in the nucleus after 60 min due to the binding of DOX to the nuclear DNA. The fluorescence of DOX-CGN was only seen in the cytoplasm after 60 min which indicates that DOX is still trapped inside the CGN particles because of the swollen state at 37 °C. At 42 °C, the fluorescence intensity in cells was increased for both free DOX and DOX-CGN after 30 min. The reason for the higher DOX levels in cells at 42 °C is unknown, but presumably it is due to increased cellular endocytosis, which has been shown to be both energy- and temperature-dependent.[2,38,39] In addition, the fluorescence intensity in the nucleus was increased for both free DOX and DOX-CGN. These results suggest that DOX was released from the CGN in the endosome and transported to the nucleus owing to the shrinkage of the nanogel upon heating.

The cytotoxicity of DOX-CGN is much less than free DOX at 37 °C (Figure 5, *C*) but comparable to free DOX at 42 °C (Figure 5, *D*). The empty CGN is not toxic to cells and heating of cells to 42 °C for 30 min does not reduce cell viability. Therefore, the increased cytotoxicity of DOX-CGN was due to the faster DOX release from the endosome. This enhancement of cytotoxicity of DOX-CGN result is in accordance with the result of DOX release behavior from DOX-CGN inside the cells.

We next examined the effects of irradiation on DOX uptake, subcellular localization and cytotoxicity in LLC1 cells exposed to DOX-CGN. The presence of DOX fluorescence (Figure 6, *A* and *B*) in the nucleus of the irradiated cells, but in the cytoplasm of non-irradiated cells suggests that DOX was not released from the CGN until irradiated with NIR light. The cytotoxic study (Figure 6, *C* and *D*) showed that only irradiation or CGN treatment or a combination of both treatments had no direct effect on cell viability. About 23% cytotoxicity was observed in non-irradiated DOX-CGN treated cells, which might be caused by the leakage release of DOX as shown in the DOX release experiment (Figure 4, *B* and *C*). A significant increase of about 26% in cytotoxicity was observed in irradiated cancer cells, but not in non-irradiated cells incubated with DOX-CGN. These results indicated that DOX-CGN release could be triggered by NIR inside live cells.

In summary, we have prepared a uniformly dispersed thermosensitive graphene nanogel, CGN, which displayed high photothermal properties and reversible dramatic size reduction with temperature increase. This CGN nanoplatform could load the anticancer drug and controlled drug release upon NIR irradiation, but was not toxic to cells at 37 °C or 42 °C. The NIR-triggered drug release of DOX-CGN inside the cells was confirmed by subcellular localization and cytotoxic test in live cancer cells. Collectively, these results show that the CGN developed here has the potential for noninvasive remote-controlled drug release triggered by exposure to light from an NIR laser. Upon exposure to the NIR laser, the light was absorbed and converted to heat through the photothermal response of graphene, which raises the temperature of the nanogel causing it to shrink and release the drug. When the laser is turned off, the drop in temperature allows the nanogel to return to its swollen state thereby stopping DOX release.

Supplementary Material

Refer to Web version on PubMed Central for supplementary material.

Acknowledgments

We acknowledge the assistance of the Lisa Muma Weitz Laboratory for Advanced Microscopy and Cell Imaging at USF Health.

This work is supported by grants 1R41CA139785 and 5R01CA152005 from the National Institutes of Health awarded to SM.

References

1. Yavuz MS, Cheng YY, Chen JY, et al. Gold nanocages covered by smart polymers for controlled release with near-infrared light. Nat Mater. 2009; 8(12):935–9. [PubMed: 19881498]
2. Sherlock SP, Tabakman SM, Xie LM, Dai HJ. Photothermally enhanced drug delivery by ultrasmall multifunctional FeCo/graphitic shell nanocrystals. ACS Nano. 2011; 5(2):1505–12. [PubMed: 21284398]
3. Lu J, Choi E, Tamanoi F, Zink JI. Light-activated nanoimpeller-controlled drug release in cancer cells. Small. 2008; 4(4):421–6. [PubMed: 18383576]

4. Hoare T, Santamaria J, Goya GF, et al. A magnetically triggered composite membrane for on-demand drug delivery. Nano Lett. 2009; 9(10):3651–7. [PubMed: 19736912]
5. Thomas CR, Ferris DP, Lee JH, et al. Noninvasive remote-controlled release of drug molecules in vitro using magnetic actuation of mechanized nanoparticles. J Am Chem Soc. 2010; 132(31): 10623–5. [PubMed: 20681678]
6. Li WY, Cai X, Kim CH, et al. Gold nanocages covered with thermally-responsive polymers for controlled release by high-intensity focused ultrasound. Nanoscale. 2011; 3(4):1724–30. [PubMed: 21321760]
7. Santini JT, Cima MJ, Langer R. A controlled-release microchip. Nature. 1999; 397(6717):335–8. [PubMed: 9988626]
8. Grayson ACR, Choi IS, Tyler BM, et al. Multi-pulse drug delivery from a resorbable polymeric microchip device. Nat Mater. 2003; 2(11):767–72. [PubMed: 14619935]
9. Markovic ZM, Harhaji-Trajkovic LM, Todorovic-Markovic BM, et al. In vitro comparison of the photothermal anticancer activity of graphene nanoparticles and carbon nanotubes. Biomaterials. 2011; 32(4):1121–9. [PubMed: 21071083]
10. Yang K, Zhang S, Zhang G, Sun X, Lee S-T, Liu Z. Graphene in mice: ultrahigh in vivo tumor uptake and efficient photothermal therapy. Nano Lett. 2010; 10(9):3318–23. [PubMed: 20684528]
11. Tian B, Wang C, Zhang S, Feng LZ, Liu Z. Photothermally enhanced photodynamic therapy delivered by nanographene oxide. ACS Nano. 2011; 5(9):7000–9. [PubMed: 21815655]
12. Yang K, Hu LL, Ma XX, et al. Multimodal imaging guided photothermal therapy using functionalized graphene nanosheets anchored with magnetic nanoparticles. Adv Mater. 2012; 24(14):1868–72. [PubMed: 22378564]
13. Wu GH, Milkhailovsky A, Khant HA, Fu C, Chiu W, Zasadzinski JA. Remotely triggered liposome release by near-infrared light absorption via hollow gold nanoshells. Journal of the American Chemical Society. 2008; 130(26):8175. [PubMed: 18543914]
14. Yang K, Wan J, Zhang S, Zhang Y, Lee S-T, Liu Z. In vivo pharmacokinetics, long-term biodistribution, and toxicology of pegylated graphene in mice. ACS Nano. 2011; 5(1):516–22. [PubMed: 21162527]
15. Yang XY, Wang YS, Huang X, et al. Multi-functionalized graphene oxide based anticancer drug-carrier with dual-targeting function and pH-sensitivity. J Mater Chem. 2011; 21(10):3448–54.
16. Lo C-W, Zhu D, Jiang H. An infrared-light responsive graphene-oxide incorporated poly(N-isopropylacrylamide) hydrogel nanocomposite. Soft Matter. 2011; 7(12):5604–9.
17. Sahu A, Choi WI, Tae G. A stimuli-sensitive injectable graphene oxide composite hydrogel. Chem Commun. 2012; 48(47):5820–2.
18. Shiotani A, Mori T, Niidome T, Niidome Y, Katayama Y. Stable incorporation of gold nanorods into N-isopropylacrylamide hydrogels and their rapid shrinkage induced by near-infrared laser irradiation. Langmuir. 2007; 23(7):4012–8. [PubMed: 17311430]
19. Sershen SR, Westcott SL, Halas NJ, West JL. Temperature-sensitive polymer-nanoshell composites for photothermally modulated drug delivery. J Biomed Mater Res. 2000; 51(3):293–8. [PubMed: 10880069]
20. Sershen SR, Westcott SL, West JL, Halas NJ. An opto-mechanical nanoshell-polymer composite. Applied Physics B-Lasers and Optics. 2001; 73(4):379–81.
21. Wang C, Flynn NT, Langer R. Controlled structure and properties of thermoresponsive nanoparticle–hydrogel composites. Advanced Materials. 2004; 16(13):1074.
22. Gorelikov I, Field LM, Kumacheva E. Hybrid microgels photoresponsive in the near-infrared spectral range. J Am Chem Soc. 2004; 126(49):15938–9. [PubMed: 15584708]
23. Yamagata M, Kawano T, Shiba K, Mori T, Katayama Y, Niidome T. Structural advantage of dendritic poly(L-lysine) for gene delivery into cells. Bioorg Med Chem. 2007; 15(1):526–32. [PubMed: 17035030]
24. Bao H, Pan Y, Ping Y, et al. Chitosan-functionalized graphene oxide as a nanocarrier for drug and gene delivery. Small. 2011; 7(11):1569–78. [PubMed: 21538871]
25. Stankovich S, Dikin DA, Dommett GHB, et al. Graphene-based composite materials. Nature. 2006; 442(7100):282–6. [PubMed: 16855586]

26. Sun X, Liu Z, Welsher K, et al. Nano-graphene oxide for cellular imaging and drug delivery. Nano Research. 2008; 1(3):203–12. [PubMed: 20216934]
27. Song P, Zhang XY, Sun MX, Cui XL, Lin YH. Synthesis of graphene nanosheets via oxalic acid-induced chemical reduction of exfoliated graphite oxide. Rsc Advances. 2012; 2(3):1168–73.
28. Kam NWS, O'connell M, Wisdom JA, Dai HJ. Carbon nanotubes as multifunctional biological transporters and near-infrared agents for selective cancer cell destruction. Proc Natl Acad Sci U S A. 2005; 102(33):11600–5. [PubMed: 16087878]
29. Zhou FF, Xing D, Ou ZM, Wu BY, Resasco DE, Chen WR. Cancer photothermal therapy in the near-infrared region by using single-walled carbon nanotubes. Journal of Biomedical Optics. 2009; 14(2)
30. Robinson JT, Welsher K, Tabakman SM, et al. High performance in vivo near-IR (> 1 mu m) imaging and photothermal cancer therapy with carbon nanotubes. Nano Research. 2010; 3(11): 779–93. [PubMed: 21804931]
31. Ghosh S, Dutta S, Gomes E, et al. Increased heating efficiency and selective thermal ablation of malignant tissue with DNA-encased multiwalled carbon nanotubes. ACS Nano. 2009; 3(9):2667–73. [PubMed: 19655728]
32. Robinson JT, Tabakman SM, Liang YY, et al. Ultrasmall reduced graphene oxide with high near-infrared absorbance for photothermal therapy. J Am Chem Soc. 2011; 133(17):6825–31. [PubMed: 21476500]
33. Kang HZ, Trondoli AC, Zhu GZ, et al. Near-infrared light-responsive core-shell nanogels for targeted drug delivery. ACS Nano. 2011; 5(6):5094–9. [PubMed: 21542633]
34. Shi FH, Ding JX, Xiao CS, et al. Intracellular microenvironment responsive PEGylated polypeptide nanogels with ionizable cores for efficient doxorubicin loading and triggered release. J Mater Chem. 2012; 22(28):14168–79.
35. Oishi M, Hayashi H, Michihiro ID, Nagasaki Y. Endosomal release and intracellular delivery of anticancer drugs using pH-sensitive PEGylated nanogels. J Mater Chem. 2007; 17(35):3720–5.
36. You J, Shao RP, Wei X, Gupta S, Li C. Near-infrared light triggers release of paclitaxel from biodegradable microspheres: photothermal effect and enhanced antitumor activity. Small. 2010; 6(9):1022–31. [PubMed: 20394071]
37. Yan B, Boyer JC, Habault D, Branda NR, Zhao Y. Near infrared light triggered release of biomacromolecules from hydrogels loaded with upconversion nanoparticles. J Am Chem Soc. 2012; 134(40):16558–61. [PubMed: 23013429]
38. Goldenthal KL, Pastan I, Willingham MC. Initial steps in receptor-mediated endocytosis — the influence of temperature on the shape and distribution of plasma-membrane clathrin-coated pits in cultured mammalian-cells. Exp Cell Res. 1984; 152(2):558–64. [PubMed: 6144562]
39. Kam NWS, Liu ZA, Dai HJ. Carbon nanotubes as intracellular transporters for proteins and DNA: an investigation of the uptake mechanism and pathway. Angew Chem Int Ed. 2006; 45(4):577–81.

Appendix A. Supplementary data

Supplementary data to this article can be found online at http://dx.doi.org/10.1016/j.nano.2013.01.003.

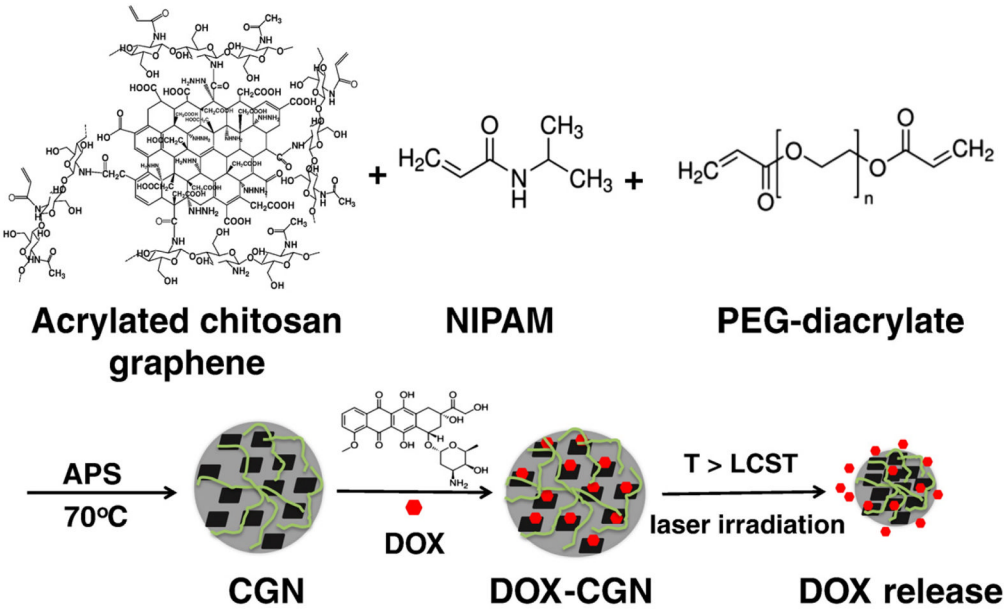

Figure 1.
A schematic of DOX-CGN synthesis and DOX release.

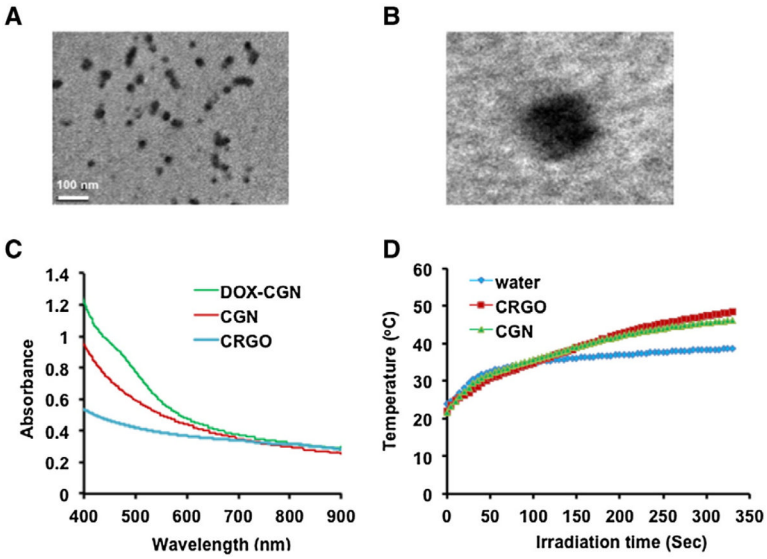

Figure 2.

(A) Transmission electron microscopy (TEM) images of CGN; **(B)** higher magnification of CGN; **(C)** UV–visible NIR spectrum of CGN, DOX-CGN and CRGO; **(D)** photothermal heating curves of water (blue), CRGO (red) suspension (25 μg/ml) and TGN (green) suspension (CRGO concentration is 25 μg/ml) exposed to 808 nm laser at a power density of 900 mW/cm^2. The temperature was measured by a thermocouple at the indicated time-points.

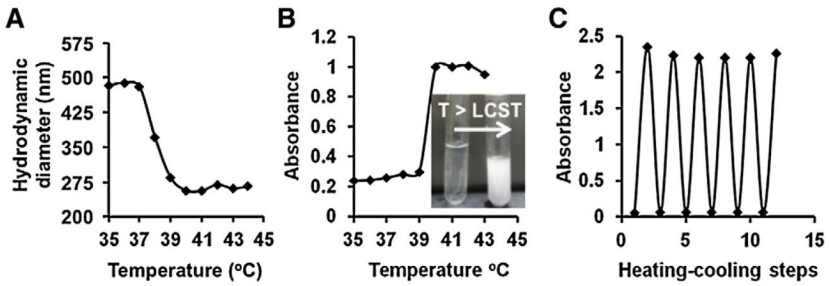

Figure 3.

(A) Temperature dependence of hydrodynamic diameter of CGN; **(B)** absorbance at 650 nm of CGN at various temperatures; and **(C)** absorbance at 650 nm of CGN after multiple heating/cooling steps.

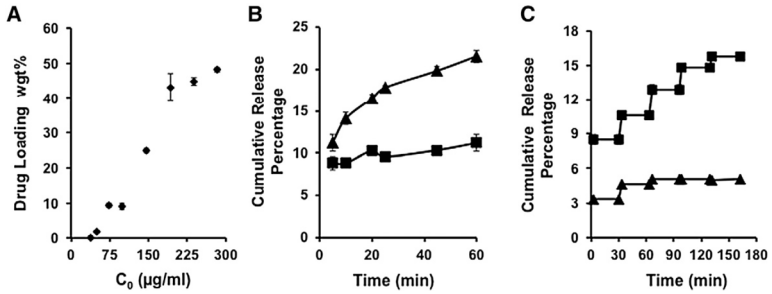

Figure 4.

(A) Drug loading as percentage of CGN, C_0 is the initial concentration of DOX solution; **(B)** In vitro drug-release profiles from DOX-CGN at 42 °C (▲) or 37 °C (■); and **(C)** NIR-light-triggered release of DOX from DOX-CGN. The DOX-CGN suspension was irradiated with (■) or without (▲) the NIR laser and the released DOX was measured with UV–vis at 485 nm.

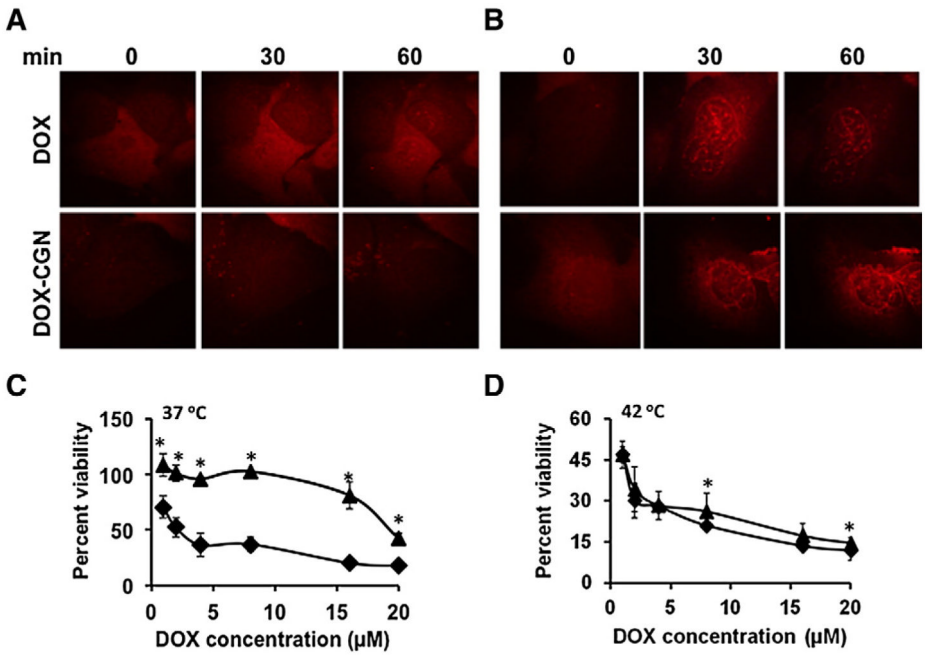

Figure 5.

Confocal microscopic images of DOX or DOX-CGN treated TRAMP-C1 cancer cells at 37 °C **(A)**, or 42 °C **(B)**. Viability of TRAMP-C1 cells treated with different concentrations of DOX (◆) or DOX-CGN (▲) at 37 °C for 72 h **(C)** (**P*<0.05, DOX versus DOX-CGN treated cells), or 42 °C for 30 min then 37 °C for 72 h **(D)** (**P*<0.05, DOX versus DOX-CGN treated cells).

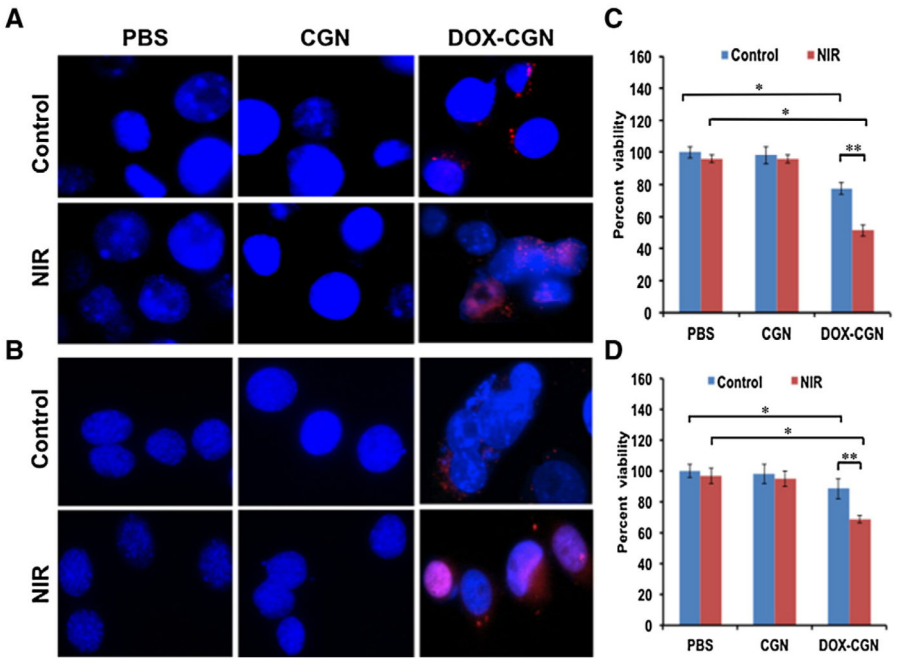

Figure 6.

Confocal microscopic images of LLC1 **(A)** and TRC1 **(B)** cells and cytotoxicity of LLC1 cells **(C)** and TRAMP-C1 cells **(D)** incubated with PBS, CGN, DOX-CGN in the presence and absence of NIR irradiation. Cells were incubated with DOX-CGN, CGN or PBS and then irradiated with an NIR laser one time at an output power of 900 mW/cm^2 for 3 min. Data are presented as the mean±standard deviation (SD) of triplicate measurements. *P<0.05 DOX-CGN groups compared to PBS groups; **P<0.01 DOX-CGN with NIR versus control.